Engineering Research (2026)90:25
https://doi.org/10.1007/s10010-026-00959-7

ORIGINALARBEITEN/ORIGINALS

Model-based prediction of normal contact stiffness values for bolted joints

Rasim Dalkiz[1] · Esmaeil Nouri Zamanabadi[1] · Georg Jacobs[1] · Stefan Wischmann[1]

Received: 24 November 2025 / Accepted: 17 July 2026
© The Author(s) 2026, modified publication 2026

Abstract

Virtual testing of a technical product with respect to its acoustic behavior enables engineers to evaluate the design without the need for physical prototypes. In order to virtually test the acoustic behavior, the effects of both, the dynamic excitations of the system and the transfer behavior of sound from the excitation source to the user must be considered in simulation models. The transfer path is primarily influenced by resonance frequencies and damping. In structures connected via bolted joints, damping within the joint is the dominant source of damping along the transfer path. Therefore, appropriate structural dynamic models of bolted joint stiffness and damping are necessary. These models must represent both the normal and tangential stiffness and damping in bolted joints. Currently, experimental investigations are still required for the parameterization of bolted joint models. As an example, for the normal behavior, optical 3D measurements of the joint surfaces are conducted to obtain their topology. The surface topology is then used to identify parameters of an exponential contact law through elasto-plastic material modeling. To eliminate the need for complex measurements during model parameterization, this article presents a method for predicting the normal contact stiffness in bolted joints based on numerically generated surfaces. For this purpose, an algorithm is implemented to generate surfaces with different roughness properties. Based on these surfaces, the exponential contact law through elasto-plastic material modeling is performed. This calculation is used to determine the contact stiffness at different pressures. A Design of Experiments is conducted in which the surface roughness is varied to calculate the normal contact stiffness. Therefore, the surface parameters S_A, S_{sk} and S_{ku} are varied. S_A describes the average roughness and thus the size of the real contact area, S_{sk} characterizes the asymmetry of the height distribution and provides information on load-bearing peaks or valleys, and S_{ku} quantifies the sharpness of the distribution and thus the proportion of peaks. These properties significantly determine the microscopic deformation at the contact and therefore directly affect the stiffness and damping values of bolted joints. The resulting normal contact stiffness values are then used to create a regression model. This makes it possible, for the first time, to derive normal contact stiffness values for different surface roughnesses without performing any physical measurements. The normal contact stiffness values calculated from the regression model are used to parameterize a structural dynamic finite element model of the Brake-Reuß-Beam bolted structure. The model predicts the eigenfrequencies with a deviation of about 1.9% compared to experimental results, confirming the accuracy of the proposed approach.

1 Introduction

The purchasing decision of customers of technical products is significantly influenced by the product's acoustic properties [1], which are often referred to as Noise, Vibration, and harshness (NVH). The term NVH is defined by the interaction between dynamic excitations, such as gear mesh excitations, and the transfer path from the location of the excitation to the receiver. In the context of a passenger vehicle, this would be the driver's ear [2]. The NVH behavior of the transfer path is largely determined by resonance frequencies and damping. The damping in transfer paths is predominantly influenced by friction in bolted joints, rather than material damping of the parts [3]. As numerical methods such as finite elements (FE) are established tools to shorten development processes, developing FE-methods to model the structural dynamic behavior is crucial for a target-oriented NVH-design. In order to avoid the necessity for time-consuming and expensive physical prototypes, NVH optimization has to be conducted using simulation models, which have to capture the effects of friction in bolted

✉ Rasim Dalkiz
rasim.dalkiz@imse.rwth-aachen.de

[1] RWTH Aachen University, Aachen, Deutschland

Published online: 11 August 2026

joints to be suitable for NVH optimization. While numerous high-fidelity models of the frictional effects in bolted joint exist [4–6], these models require the identification of stiffness and damping which can usually only by obtained experimentally. As an illustrative example for the characterization of the normal behavior, optical 3D measurements of the joint surfaces are carried out in order to capture the surface topology. The measured surface topology is used to identify the parameters of an exponential contact law, which is subsequently determined using elasto-plastic material modeling [3]. This process is time-consuming and costly because it requires a 3D surface profile of the physical prototype of the bolted joint, as surface roughness parameters are not sufficient. At the same time, the influence of the surface profile on the stiffness and damping of the bolted joint should not be neglected. Therefore, this article presents a model-based approach that evaluates the influence of surface topography on normal behavior and predicts normal contact stiffness. This method is used for steel-steel contact. An algorithm is implemented to generate different numerical surfaces.

In Section 2, a brief overview over the state of the art of rough surface contact modeling is presented. Section 3 describes the proposed method of generating surfaces numerically, calculating contact stiffness, and considering surface pairings with different stiffness levels. Furthermore, a design of experiments (DoE) for the numerical surfaces is carried out based on the presented method. The results are then used to create a regression model that predicts normal contact stiffnesses for the three specified surface values. The normal contact stiffnesses predicted by the regression model are compared with normal contact stiffnesses calculated on the basis of 3D surface measurements. In Section 4 the results are presented, where the normal contact stiffness values calculated from the regression model are used to parameterize a structural dynamic finite element model of the Brake-Reuß-Beam (BRB) bolted structure to predict eigenfrequencies. The results are compared to measurements. There-after, concluding remarks and aspects of further work will be presented in section 5.

2 State of the art

In what follows, an overview over rough surface contact modeling is given. Furthermore, an overview over surface roughness value is given and the influence of surface roughness values on the normal contact stiffness is discussed.

The mechanical interactions between contacting surfaces are relevant in various engineering disciplines, including tribology and structural dynamics. Numerous models have been proposed to characterize rough-surface contact. Greenwood and Williamson [5] analyzed the contact between a rough surface and a rigid, flat surface, modeling the roughness as a set of asperities with Gaussian height distribution. Based on this probabilistic representation of the surface topography, the Greenwood-Williamson model provides a deterministic formulation for calculating contact stiffness and real contact area. Greenwood and Tripp [6] extended this approach to the case of two rough surfaces, by introducing the concept of an equivalent combined roughness derived from the convolution of both surface height distributions. The investigations reveals that the real contact area increases with the applied load in a nonlinear manner, governed by the statistical properties of the combined roughness and the local asperity slopes, rather than following a strict proportionality. Greenwood and Williamson [5] further introduced a plasticity index Ψ, defined by material hardness, effective modulus, surface roughness, and asperity curvature. They reported elastic deformation for $\Psi < 0.6$, plastic deformation for $\Psi > 1$, and transitional behavior in the intermediate range [7]. Bush, Gibson, and Thomas [8] expanded the Greenwood and Williamson analysis [4] by including statistical distributions of asperity radii in addition to height distributions [7]. These approaches are based on the assumptions of elastic deformation and Gaussian height distributions. To account for deviations from these assumptions, subsequent models addressed non-Gaussian surface statistics and plastic deformation. McCool [7] modified the Greenwood and Williamson framework to incorporate non-Gaussian roughness and plasticity. Additional work provided 3D analyses of elastic-plastic behavior in the case of non-Gaussian surfaces [8]. Majumdar and Bhushan [9, 10] developed fractal-based models of rough surface contact, and Persson [6] proposed a scale-dependent theory of contact mechanics for randomly rough surfaces, which enables prediction of real contact area and pressure distribution without reference to discrete asperities. Research on elastic-plastic contact has primarily relied on numerical methods or hybrid approaches that combine elasticity theory with approximations for plastic deformation and non-Gaussian surface characteristics [11, 12]. The micro-contact analysis module in AVL Excite [13] applies a exponential contact law according to Greenwood and Tripp model [8] to 3D surface topographies [12] and includes extensions for elastic-plastic contact behavior. Surface profiles for such analyses can be obtained either from profilometer measurements or through synthetic generation [14–16].

The contact models are largely based on the actual surface topography, particularly on the distribution and geometry of asperities. To enable an accurate characterization of the surface, the following section presents the relevant surface roughness parameters. In general, the topography of technical surfaces can be described with long- and short-wavelength components. Long-wavelength components, of-

ten referred to as waviness, are typically related to the manufacturing process, tool paths, or macroscopic form deviations. Short-wavelength components, referred to as roughness, capture the fine-scale asperities that dominate contact mechanics and load-bearing behavior.

To quantify surface topography, a range of areal surface parameters have been standardized in ISO 25178 [17].

The arithmetical mean height S_a represents the mean of the absolute height deviations from the mean plane over the entire evaluation area. Mathematically, it is defined as

$$S_A = \frac{1}{A} \iint_A z\,(x, y)\,dxdy \tag{1}$$

where z(x,y) denotes the surface height relative to the mean plane at the position (x,y), and A is the evaluation area. S_a serves as a general measure of roughness amplitude. Larger values of Sa indicate rougher surfaces with higher asperities, which typically reduce the real contact area, decrease normal stiffness, and increase the tendency toward plastic deformation.

The skewness S_{sk} characterizes the asymmetry of the surface height distribution. Negative values ($S_{sk} < 0$) indicate surfaces dominated by valleys, which may act as lubricant reservoirs and reduce the initial contact stiffness. Positive values ($S_{sk} > 0$) correspond to surfaces dominated by peaks, leading to high local stress concentrations at asperity contacts and thus to increased wear susceptibility and reduced load-bearing capacity. Figure 1 shows a schematic sketch describing S_{sk}.

Kurtosis S_{ku}: S_{ku} describes the sharpness of the surface height distribution. A Gaussian distribution corresponds to $S_{ku} = 3$. Surfaces with $S_{ku} > 3$ exhibit pronounced peaks and valleys, which result in localized contact points and stress concentrations. In contrast, surfaces with $S_{ku} < 3$ have a flatter distribution with fewer extreme asperities, leading to more uniform load distribution and higher contact stiffness. Figure 2 shows a schematic sketch describing S_{ku}.

Investigations have also addressed the influence of surface roughness parameters on normal contact response. Amplitude parameters, parameters describing the shape of the height distribution, and hybrid parameters have been identified as relevant for surface contact [18]. The effect of the root mean square value of the surface height distribution on

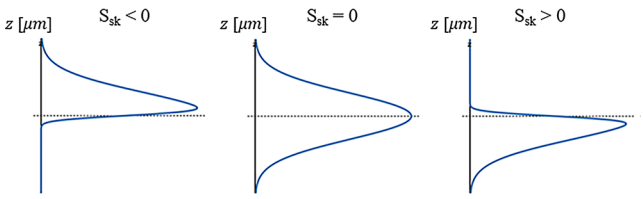


Fig. 1 Description of skewness

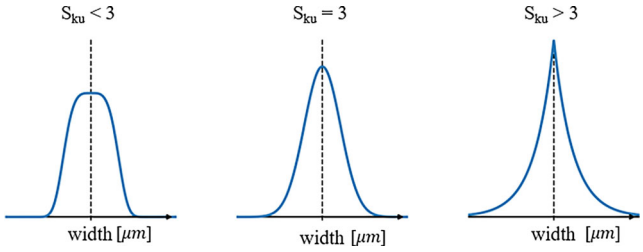


Fig. 2 Illustration of surface height distributions with varying kurtosis (S_{ku})

normal contact stiffness has been analyzed, with results indicating that larger RMS values reduce stiffness in elastic-plastic contact [19]. Combined numerical and experimental studies have shown that increasing contact pressure and smoother surfaces lead to higher interface stiffness [20]. Further analyses have examined the role of skewness and kurtosis of surface height distributions in contact mechanics [21].

The deformation of surface asperities determines the normal contact stiffness, linking the surface topography to the mechanical response of the interface. Since the normal contact stiffness defines the mechanical coupling between components, it significantly affects the structural dynamic behavior of assemblies, influencing natural frequencies, mode shapes, and damping characteristics. Variations in contact stiffness can lead to noticeable frequency shifts and amplitude changes, particularly in systems with bolted or frictional joints where contact conditions dominate the overall dynamic response. Polycarpou et al. [8] demonstrated this correlation by measuring and modeling normal contact stiffness and damping at the meso scale, showing that changes in contact stiffness result in measurable shifts of eigenfrequencies. Similarly, Ren et al. [9] and Zhang et al. [10] developed numerical and experimental approaches to identify contact stiffness from modal data and to quantify its influence on vibration characteristics, confirming the strong interrelation between surface topography, contact mechanics, and structural dynamics.

In the following, the modeling approach used in the validation is explained to determine joint stiffness in structural dynamic analyses. Zero-thickness elements (ZTE) represent an approach in finite element modeling to describe the structural dynamic behavior of joints. They are formulated as linear hexahedral elements with no geometric extent in the direction of the contact normal, such that opposing nodes are located directly on top of each other. Despite their lack of geometric thickness, they enable the representation of nonlinear contact properties. For example, joint stiffness and damping can be evaluated for structural dynamic analyses. In the normal direction, an exponential behavior is typically assumed, while in the tangential direction a degressive stiffness characteristic is modeled. By coupling normal and

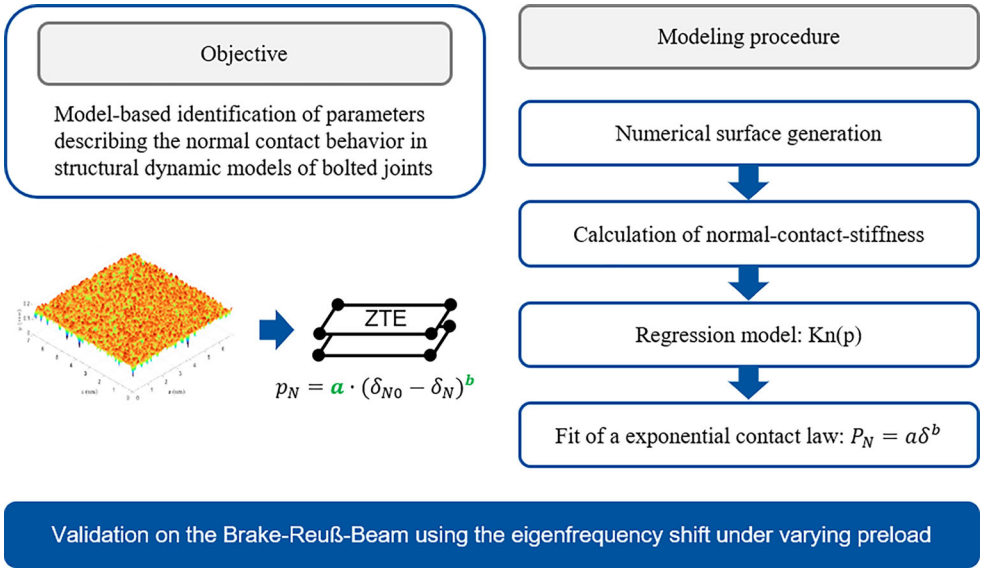


Fig. 3 Methodological approach for model-based identification of finite element parameters in structural dynamic behavior models

tangential behavior, both preload effects and the transition from micro-slip to macro-slip can be captured depending on the ratio between tangential stress and the friction limit.

3 Method

The contact models introduced in Section 2 can be employed to parameterize the normal contact behavior in structural dynamic models of bolted joints. The normal contact behavior in bolted joints can be described by an exponential contact law, as illustrated in Fig. 3 the Zero-Thickness-Element (ZTE) is using such a law [6]. This law defines the contact pressure as a function of the normal penetration. The parameters to be identified, a and b, are highlighted in green in Fig. 3. However, determining these parameters typically requires a 3D surface measurement of the contact area and, therefore, a physical prototype. To overcome this limitation, the following method provides a model-based approach that enables the prediction of the parameters a and b without the need for experimental surface data. The workflow of this approach is shown in Fig. 3. First, surface topographies are numerically generated. Therefore, suitable surface parameters are selected that collectively capture the influence of surface topography on contact stiffness. The parameters S_a, S_{sk}, and S_{ku} are found to be particularly suitable for this purpose. The input parameters for this surface generation are the surface roughness values S_a, S_{sk}, and S_{ku}. Subsequently, a contact analysis is carried out using the Micro-Contact Analysis Tool in AVL to determine the normal contact stiffness at different nominal pressures. To quantify the influence of the three surface roughness values on the normal contact stiffness, a Latin Hypercube Sampling scheme is implemented. A total of 36 design points are selected within the following bounds $S_A \in [1, 9]$ µm, $S_{sk} \in [-1, 0.5]$, and $S_{ku} \in [2.5, 4.0]$. Steel is considered as the material for all simulations. Based on these design points, a regression model is established to describe the normal contact stiffness as a function of nominal pressure, the three surface roughness parameters, and the material properties. Using this regression model, the exponential contact law is fitted to three support points of the normal contact stiffness obtained at different pressures, allowing the parameters a and b to be determined.

In the following subsections, the main aspects of the method are explained. It starts with an algorithm to generate surfaces numerically. After that the calculation of the normal contact stiffness is explained. And finally, an approach the consider dissimilar surface pairs is described.

3.1 Rough surface generation

To generate rough surfaces, the three roughness parameters S_a, S_{sk} and S_{ku} outlined in section 2 are considered. These parameters were selected due to their relevance in characterizing surface topography.

Roughness samples are generated according to the procedure described in [15]. The method is based on an initial statistical distribution of asperities, as shown in Fig. 4a. Each asperity is described by the index i and has a height $k_p(i)$ and a base diameter $D(i)$. The asperities are truncated at the top with a diameter of $d\,(i) = 0.1 \cdot D(i)$. The side-

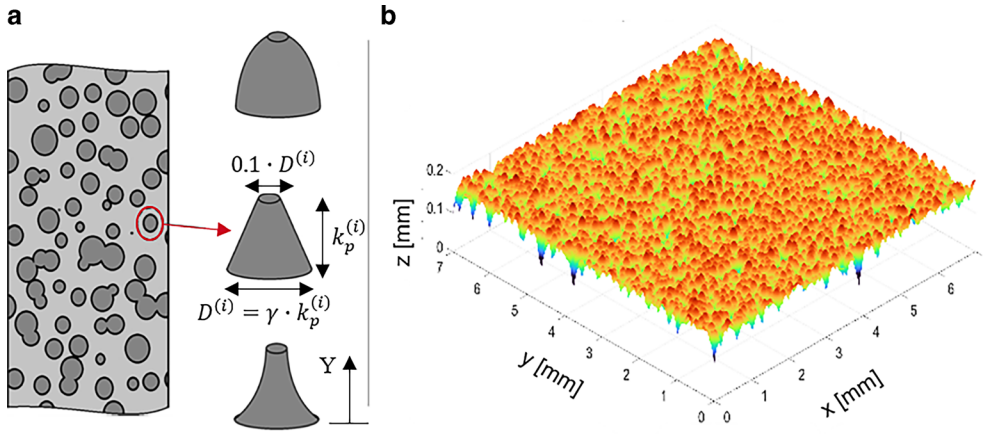


Fig. 4 Method for the numerical generation of surfaces

wall profile of each element is defined as a function of the wall-normal coordinate Y,

$$Y = k_p(i)\left[1 - \left(\frac{r - d\,(i)\,/2}{D(i)/2 - d(i)/2}\right)^n\right] \tag{2}$$

the radial distance from the element center r, and the exponent n, which determines the overall element shape. For the optimization of rough surfaces, the implementation provided in the GitHub repository [17] is employed. The tool applies a Weibull distribution for the element heights and optimizes its scale and shape parameters, using a genetic algorithm. This enables the generation of surfaces with prescribed roughness characteristics. In the present work, the tool is used to optimize surface parameters such that the resulting surfaces matched the target roughness statistics (S_a, S_{sk}, S_{ku}). One example for a generated surface is shown in Fig. 4b. As a result, height matrices, which contain the height and position of the asperities, can be extracted for each surface for further investigations.

3.2 Normal contact analysis and regression model

To determine the relationship between the numerically generated surface topographies and the resulting pressure dependent normal contact stiffness, a contact analysis is performed using the *Micro-Contact Analysis Tool* by AVL. This simulation enables the evaluation of how surface roughness parameters influence the normal contact stiffness under varying loading conditions. After generating paired surfaces, the corresponding height matrices are extracted for subsequent normal contact analysis. Simulations are conducted using *Micro-Contact Analysis* tool by AVL, which considers the elastoplastic deformation of individual asperities. This enables the computation of the real contact area and the corresponding local pressure distribution directly from measured or generated surface topographies. The surfaces are assigned material properties corresponding to steel (Young's modulus: 210.000 MPa; surface hardness: 4000 MPa; Poisson's ratio: 0.33). Each surface measures $7 \times 7\,mm^2$ with a spatial resolution of 7 µm in the x-y-plane. To preserve the prescribed statistical roughness parameters, no filtering is applied. Contact simulations are performed for the surface pairs and pressure penetration curves are the result. An applied pressure range of 0–50 MPa is selected to capture the dominant elastic-plastic regime of the contact. Due to the elastic-plastic behavior, pressure exhibit a nonlinear dependence on displacement, resulting in a nonlinear contact stiffness.

To investigate the correlation between surface roughness parameters and the resulting contact stiffness, a regression model is applied to the DoE dataset, are S_a, S_{sk}, and S_{ku} serve as input variables, and contact stiffness values at nominal pressures of 5 MPa, 25 MPa, and 45 MPa act as response

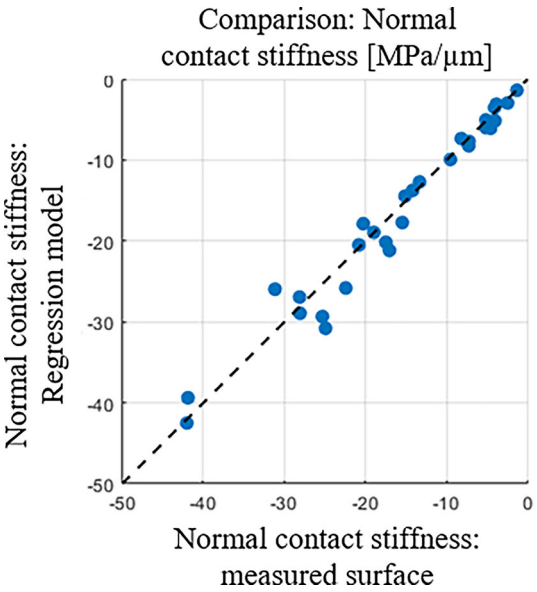


Fig. 5 Verification of the regression model using measured normal contact stiffness values

variables. Gaussian Process Regression (GPR) is employed because of its capability to handle complex regression tasks involving small sample sizes and nonlinear dependencies [21]. An exponential kernel defines the covariance structure, as it effectively represents smooth yet non-differentiable behavior typically observed in physical systems. The exact fitting method is used owing to the limited dataset size, and the kernel hyperparameters are automatically optimized through Bayesian optimization using the expected-improvement-plus acquisition function.

To verify the results from the Regression model the measured surface data are also imported into AVL, following the same procedure used for numerically generated surfaces. Contact analysis is conducted to compute the corresponding pressure-penetration curves, and contact stiffness values are evaluated at three pressure levels. These results are subsequently in Fig. 5 compared with the predictions obtained from the regression model to assess its accuracy. The average error is 16.75% for low pressures of 5 MPa and 9.5% for the highest pressure of 45 MPa. Thus, the regression model shows a valid correlation with the normal contact stiffnesses calculated from the measured surfaces.

The verified regression model is used to derive parameters for the exponential contact law. Therefore, pointwise stiffness values are extracted from the pressure-displacement curves at three representative pressure levels (5, 25 and 45 MPa). Using the contact stiffness values at the three selected pressure points, an inverse fitting procedure is employed to reconstruct the continuous relationship between contact pressure and displacement. This is achieved using the expoential contact law formulation, expressed as $P{=}a \cdot h^b$, where P denotes the contact pressure and h represents the indentation depth. By optimizing the coefficients a and b, the best-fit curve describing the contact behavior can be obtained, providing a continuous representation of the pressure-indentation response based on discrete stiffness data.

3.3 Evaluation of contact stiffness for dissimilar surfaces

The regression-based contact evaluation was initially performed for surfaces with identical S_a, S_{sk}, and S_{ku}. However, in practical applications, surfaces in contact often exhibit different roughness parameters. To account for this, an approach was implemented to evaluate the contact between dissimilar surfaces. Consider two surfaces, denoted as 1 and 2, in normal contact. These surfaces can be modeled elastic-plastic, behaving as nonlinear springs. The total normal displacement is the sum of the individual deformations of each surface:

$$\delta_{Total} = \delta_1 + \delta_2 \tag{3}$$

Differentiating this equation yields:

$$d\delta_{Total} = d\delta_1 + d\delta_2 \tag{4}$$

Assuming that the contact pressure P is uniformly distributed across the contact area, both surfaces experience the same pressure:

$$dP = dP_1 = dP_2 \tag{5}$$

The contact stiffness at a given pressure P_i is defined as the derivative of pressure with respect to displacement:

$$k = \frac{dP}{d\delta} \tag{6}$$

From this definition, the differential displacement can be expressed as:

$$d\delta_1 = \frac{dP}{k_1}, d\delta_2 = \frac{dP}{k_2}, \tag{7}$$

Substituting these expressions into the total displacement equation gives:

$$d\delta_{Total} = \frac{dP}{k_1} + \frac{dP}{k_2} \tag{8}$$

where K_{eq} is the equivalent contact stiffness, and k_1 and k_2 are the stiffnesses of surfaces 1 and 2, respectively. Dividing both sides by dP leads to:

$$\frac{d\delta_{Total}}{dP} = \frac{1}{k_1} + \frac{1}{k_2} \rightarrow K_{eq} = \frac{1}{\frac{1}{k_1} + \frac{1}{k_2}} \tag{9}$$

To apply this formulation, the stiffness of each individual surface, k_1 and k_2, must be known. These values can be extracted from the equivalent contact stiffness between similar surfaces, obtained via regression analysis of the Design of Experiments (DoE) data. Since k_1 and k_2 can be calculated from the regression model, the equivalent stiffness for dissimilar surface pairs can be determined using the above equation. This approach was employed to calculate the contact stiffness between dissimilar surfaces at pressure levels of 5 MPa, 25 MPa and 45 MPa.

3.4 Validation approach

To demonstrate the application of the presented methods, the model parameters a and b describing the normal contact behavior are determined for a bolted structure. As a representative example, the well-known BRB [3] is used, which is frequently adopted in the literature for validation of joint

Table 1 Surface values and model parameters

Parameters			
	S_A [µm]	S_{sk} [–]	S_{ku} [–]
Surface roughness	2.12	–0.5	3.84
–	–	–	–
–	a [Pa/m^b]	b [–]	–
ZTE	2.41e22	4.11	–

modeling approaches. The structure consists of two steel beam elements connected by three M8 bolts. The surface roughness parameters assumed for the contact interfaces are listed in Table 1. Based on these surface roughness parameters, the model parameters are derived from the previously developed regression model and are also summarized in Table 1. The parameters are implemented together with a Zero Thickness Element (ZTE) into a pre-existing finite element model of the BRB. Using the ZTE formulation and the identified model parameters, the normal contact behavior of the BRB can be accurately represented. Subsequently, the frequency response function (FRF) of the system is computed for bolt preload levels of 1.15 kN, 5.75 kN, and 11.5 kN. With that a quantitative evaluation of the shift in the eigenfrequencies depending on the bolt preload is possible. With the validated method, the influence of surface roughness on the normal contact stiffness can be determined in a model-based manner, and model parameters for structural dynamic models can be predicted. To validate the model parameters determined using the proposed approach, the simulation results are compared with experimental data. For this purpose, a BRB specimen made of steel was manufactured, featuring surface roughness characteristics identical to those listed in Table 1 and assumed for the parameter identification. The experimental procedure follows a well-established approach described in the literature [22]. The structure is excited using an electromagnetic shaker, while the system response is measured with a laser vibrometer. The bolt preload is monitored by means of strain gauges mounted within a borehole inside the bolt, allowing precise measurement of the tensile strain. The results of the validation are presented in Section 4.

4 Results

In the following section, the influence of the surface roughness values on the normal contact stiffness is shown, using the regression model for the normal contact stiffness from section 3. Subsequently, the developed method is validated by comparing the simulated and measured eigenfrequency shifts obtained from structural dynamic tests on the BRB. The model on which the investigations are based on is shown in Fig. 6. The model contains the BRB, which consists of two beam elements bolted together with three M8 bolts. The geometric dimensions of the beam, as well as the measurement and excitation positions, are shown in Fig. 6. The BRB is modelled as a milled aluminium part with an average surface roughness of 2 μm and constant friction coefficient μ of 0.246. Hexahedral elements with a mesh size of one millimeter are used for the parts.

As result of the regression model, it is possible to derive characteristic maps of the normal contact stiffness under different pressure levels depending on the surface roughness values. Figure 5 illustrates the predicted normal contact stiffness (K_N) as a function of the surface roughness parameters S_a, S_{sk}, and S_{ku} for nominal pressures of 25 MPa (left column) and 45 MPa (right column). The normal contact stiffness increases significantly with the applied pressure level, as expected due to the larger real contact area under higher loading conditions. For both pressure levels, the stiffness decreases with increasing roughness amplitude Sa. At a constant Sa, surfaces with negative skewness ($Ssk < 0$) and moderate kurtosis ($Sku \approx 3$) exhibit the highest contact stiffness, indicating that a surface dominated by load-

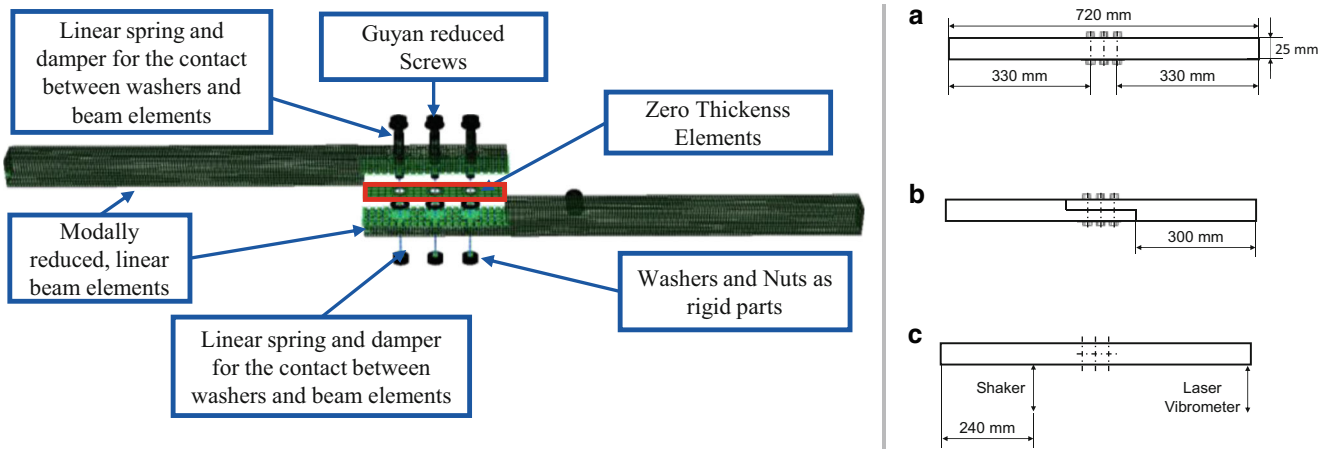


Fig. 6 Comprehensive model of the BRB

bearing peaks and moderate peak sharpness favors higher stiffness. In contrast, positive skewness (Ssk > 0) or high kurtosis values (Sku > 3.5) lead to a reduction in stiffness, as contact occurs mainly at isolated asperities with limited load-sharing capability. Quantitatively, the normalized stiffness KN ranges approximately from 5 N/m for rough, positively skewed surfaces (Ssk > 0, Sa > 7 µm) up to about 25–35 N/m for smoother, negatively skewed surfaces (Ssk ≈ –1, Sa ≈ 1 µm). The overall trend remains consistent across both pressure levels, with the 45 MPa case showing uniformly higher stiffness values by roughly 30–40% compared to 25 MPa.

The normal contact stiffness values obtained from the regression model are used to derive model parameters for the ZTE, which are subsequently applied in structural dynamic simulations. The system is excited along the bolt axis normal to the contact surface by a harmonic force of 0.6 N, and the system response is measured in terms of surface vibration velocity, known as the mechanical admittance, in the same direction. The resulting frequency response functions of the first bending mode of the BRB is shown in Fig. 7b. A clear shift of the eigenfrequency toward higher frequencies is observed with increasing bolt preload. For the lowest preload of 1.15 kN, the first bending eigenfrequency occurs at 159 Hz. Increasing the preload to 5.75 kN results in a frequency shift to around 162 Hz, while at the highest preload of 11.5 kN, the resonance peak is located at 165 Hz. This corresponds to a relative increase of 3.8% between the lowest and highest preload levels. The obtained results demonstrate that the identified model parameters are capable of accurately reproducing the stiffness increase of the joint, which manifests as a shift of the eigenfrequency toward higher values with increasing bolt preload. For validation purposes, the simulation results are compared with the experimental data. The measurement procedure is carried out according to the method described in Section 3.5. For the measurement each preload level is tested five times to ensure repeatability. The deviation in the reproducibility of the measured frequency response remains below 1%, confirming the reliability and stability of the experimental setup. Figure 8 compares the experimentally measured and numerically simulated frequency response functions of the BRB structure for three different bolt preload levels (1.15 kN, 5.75 kN, and 11.5 kN). Both the experimental and the simulated results exhibit the same qualitative trend. With increasing bolt preload, the resonance peak of the first bending mode shifts toward higher frequencies, indicating an increase in normal contact stiffness. Quantitatively, the measured resonance frequencies are 158 Hz, 162 Hz, and 165 Hz for preload levels of 1.15 kN, 5.75 kN, and 11.5 kN, respectively. The corresponding simulated eigenfrequencies are about 161 Hz, 164 Hz, and 166 Hz. The maximum deviation between simulation and experiment occurs at the lowest preload level and amounts to roughly 3 Hz, which corresponds to a relative error of about 1.9%. Across all preload levels, the average deviation remains below 2 Hz. These results confirm that the identified model parameters reliably reproduce the stiffness-dependent upward shift of the eigenfrequency. The close agreement between the simulated and experimental results confirms the validity of the proposed parameter identification approach for modeling the normal contact behavior of bolted joints.

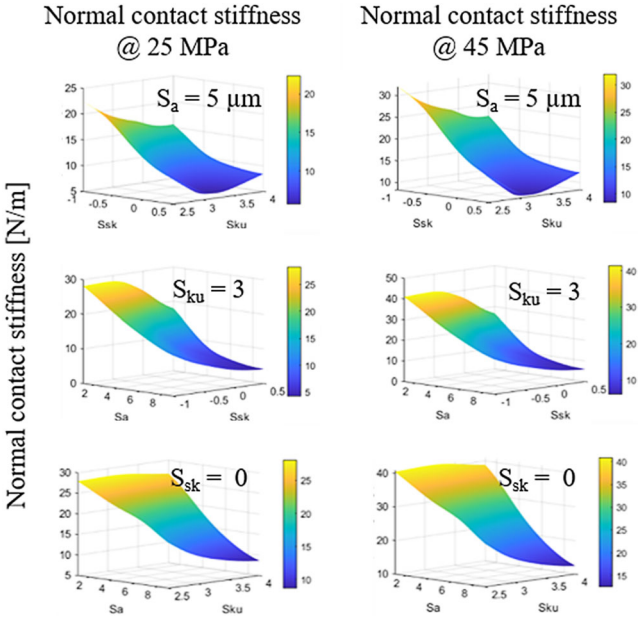


Fig. 7 Normal contact stiffness map depending on pressure distribution and surface roughness

The presented approach enables engineers to predict eigenfrequencies with a validated accuracy of 1.9% without the need for physical prototypes. Based solely on the three surface roughness parameters S_A, S_{sk}, and S_{ku}, the method provides a model-based means to efficiently and reliably assess the structural dynamic behavior of bolted joints.

5 Conclusion

To predict energy dissipation using friction models, the relative displacements within the joint must be known, as they are governed by the local contact stiffness. Consequently, the first step toward developing predictive frictional contact models is the accurate estimation of the normal contact stiffness influenced by the surface roughness characteristics. At present, the model parameters necessary to describe the normal contact stiffness are typically obtained through experimental investigations. For example, in the case of normal behavior, optical 3D measurements of joint surfaces are conducted to capture the surface topology, which is then

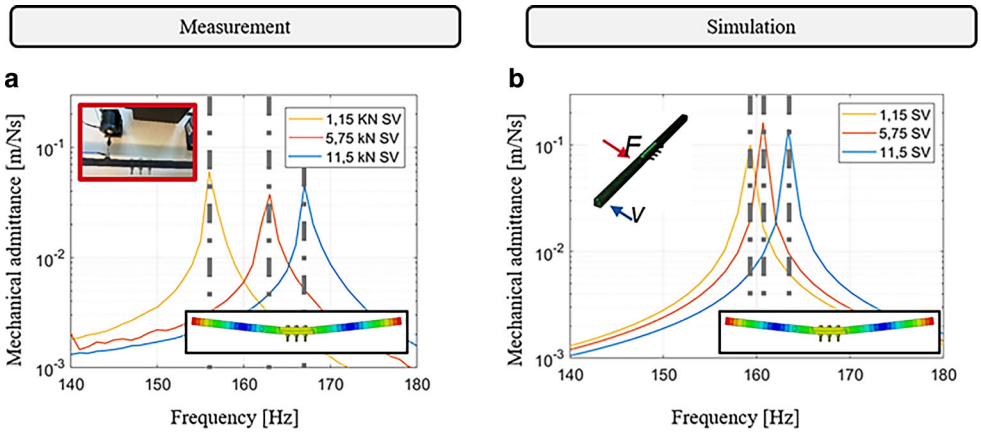


Fig. 8 Comparison of the FRF in normal direction between experiment and simulation

used to determine the parameters of an exponential contact law through elasto-plastic material modeling. To reduce the reliance on complex experimental measurements during model parameterization, this article presented a method for predicting the normal contact stiffness in bolted joints based on numerically generated surfaces.

The proposed method enables the model-based prediction of the model parameters a and b of an exponential contact law without requiring experimental surface data. Numerically generated surfaces, defined by the roughness values S_A, S_{sk}, and S_{ku}, are analyzed using contact to determine the normal contact stiffness at various nominal pressures. A Latin Hypercube Sampling with 36 design points quantifies the influence of the roughness values. Based on these results, a regression model is developed to describe the normal contact stiffness as a function of pressure, surface characteristics and material properties. The parameters a and b are then derived by fitting the exponential contact law to the stiffness data predicted by the regression model. As a result, that the normal contact stiffness can be predicted by up to 16% accuracy for lower pressure levels and 9.5% for high pressure levels.

Structural dynamic measurements were carried out on the jointed structure of the Bake-Reuß-Beam to validate the proposed method by evaluating the eigenfrequency shift with varying bolt preload. The Results shows that both simulation and experiment exhibit an upward shift of the first bending eigenfrequency with increasing preload. The maximum deviation between simulated and measured values is about 3 Hz, which is about 1.9%, confirming the method's capability to accurately predict the preload-dependent normal contact stiffness.

With the presented method and the resulting regression model for the normal contact stiffness, the engineer can evaluate the technical product in terms of its NVH behavior at an early stage of the product development process. This eliminates costly and time-consuming iterations with physical prototypes.

In further investigations, a method to predict tangential behavior of bolted joints can be developed. The results can then be used to parameterize the bolted joint model approaches without prior experimental investigation. This enables a forward model-based prediction of the acoustic behavior of bolted joints.

Funding This research has been supported by the federal Ministry for Economic Affairs and Energy within the scope of IGF project No. 01IF23266N.

Open Access funding enabled and organized by Projekt DEAL.

Data availability All data supporting the findings of this work are included in the article.

Declarations

Conflict of interest The authors declare that they have no competing interests.

Open Access Dieser Artikel wird unter der Creative Commons Namensnennung 4.0 International Lizenz veröffentlicht, welche die Nutzung, Vervielfältigung, Bearbeitung, Verbreitung und Wiedergabe in jeglichem Medium und Format erlaubt, sofern Sie den/die ursprünglichen Autor(en) und die Quelle ordnungsgemäß nennen, einen Link zur Creative Commons Lizenz beifügen und angeben, ob Änderungen vorgenommen wurden. Die in diesem Artikel enthaltenen Bilder und sonstiges Drittmaterial unterliegen ebenfalls der genannten Creative Commons Lizenz, sofern sich aus der Abbildungslegende nichts anderes ergibt. Sofern das betreffende Material nicht unter der genannten Creative Commons Lizenz steht und die betreffende Handlung nicht nach gesetzlichen Vorschriften erlaubt ist, ist für die oben aufgeführten Weiterverwendungen des Materials die Einwilligung des jeweiligen Rechteinhabers einzuholen. Weitere Details zur Lizenz entnehmen Sie bitte der Lizenzinformation auf http://creativecommons.org/licenses/by/4.0/deed.de.

References

1. Genuit K (2010) Sound-Engineering im Automobilbereich: Methoden zur Messung und Auswertung von Geräuschen und Schwingungen. Springer, Berlin, Heidelberg

2. Möser M, Kropp W (2010) Körperschall. Physikalische Grundlagen und technische Anwendungen vol 3. Springer, Heidelberg, New York
3. Brake MR (2017) Mechanics of jointed structures. Recent research-hand open challenges. Springer
4. Segalman DJ (2005) A four-parameter Iwan model for lap-type joints. J Appl Mech Asme 72(5):752–760. https://doi.org/10.1115/1.1989354
5. Gaul L, Mayer M (2008) Modeling of Contact Interfaces in Built-up Structures by Zero-thickness Elements. In: IMAC XXVI
6. Mayer M (2007) Zum Einfluss von Fügestellen auf das dynamische Verhalten zusammengesetzter Strukturen. Zugl.: Stuttgart, Univ., Diss.,2007. Der Andere Verl, Tönning
7. Wischmann S, Berroth J, König F, Jacobs G (2023) An improved method for fem modelling and parameter identififcation of damping in bolted lap joints using Zero-thickness Elements. Icsv29 29th Int Congr Sound Vib
8. Shi X, Polycarpou A (2005) Measurement and Modeling of Normal Contact Stiffness and Contact Damping at the Meso Scale. Journal of Vibration and Acoustics 127:52–60. https://doi.org/10.1115/1.1857920
9. Greenwood JA, Williamson JBP (1966) Contact of Nominally Flat Surfaces. Proc Math Phys Eng Sci 295:300–319. https://doi.org/10.1098/rspa.1966.0242
10. Bush AW, Gibson RD, Thomas TR (1975) The Elastic Contact of a Rough Surface. Wear 35:87–111. https://doi.org/10.1016/0043-1648(75)90145-3
11. Kim TW, Bhushan B, Cho YJ (2006) The Contact Behavior of Elastic–Plastic Non-Gaussian Rough Surfaces. Tribology Letters 22(1):1–15. https://doi.org/10.1007/s11249-006-9036-5
12. Kogut L, Etsion I (2002) Elastic–Plastic Contact Analysis of a Sphere and a Rigid Flat. Journal of Applied Mechanics 69(5):657–662. https://doi.org/10.1115/1.1490373
13. AVL EXCITE, AVL List GmbH (Jahr) AVL EXCITE™ – Simulation of Powertrain Dynamics. https://www.avl.com. Accessed 8 Apr 2026
14. Paggi M, Ciavarella M (2010) Rough Surface Contact Modelling—A Review. Meccanica 45:751–765. https://doi.org/10.1007/s11012-010-9321-0
15. M. Paggi, M. Ciavarella. A Review of Elastic–Plastic Contact of Rough Surfaces: Theoretical Approaches and Applications. Contact Mechanics and Tribology Journal, 2015.
16. Minet R, Francisco A, Brunetière N (2016) A Review of Methods of Random Surface Topography Modeling. Tribology International 103:469–482
17. International Organization for Standardization (2012) ISO 25178-2:2012. Geometrical Product Specifications (GPS) – Surface Texture: Areal – Part 2: Terms, Definitions and Surface Texture Parameters. International Organization for Standardization, Geneva, Switzerland
18. Francisco A, Brunetière N (2016) A Hybrid Method for Fast and Efficient Rough Surface Generation. Pro Inst Mech Eng Part J J Eng Tribol 230(7):747–768. https://doi.org/10.1177/1350650115612116
19. Xu Y, Zhang X, Ren Z, Zhang W (2020) Estimation of the Normal Contact Stiffness for Frictional Interfaces in Sticking and Sliding Conditions. Tribol Int 146:106234. https://doi.org/10.1016/j.triboint.2019.106234
20. Belhadjamor M, Belghith S, Mezlini S, El Mansori M (2020) Numerical Study of Normal Contact Stiffness: Non-Gaussian Roughness and Elastic–Plastic Behavior. Pro Inst Mech Eng Part J J Eng Tribol. https://doi.org/10.1177/1350650119893520
21. Pan T, Cai Y, Chen S (2021) Development of an Engine Calibration Model Using Gaussian Process Regression. Int.J Automot. Technol. 22(2):327–334. https://doi.org/10.1007/s12239-021-0031-5
22. Wischmann S, Seifert K, Berroth J, Jacobs G (2022) On the influence of surface sealant on the nonlinear dynamics of jointed structures. Mech Syst Signal Process 173:109061. https://doi.org/10.1016/j.ymssp.2022.109061
23. Persson BNJ (2006) Contact Mechanics for Randomly Rough Surfaces. Surface Science Reports 61:201–227. https://doi.org/10.1016/j.surfrep.2006.04.001
24. McCool J (2000) Extending the Capability of the Greenwood–Williamson Microcontact Model. Journal of Tribology 122(3):496–502. https://doi.org/10.1115/1.555392

Publisher's Note Springer Nature remains neutral with regard to jurisdictional claims in published maps and institutional affiliations.